

Toroidal-Spiral Particles for Codelivery of Anti-VEGFR-2 Antibody and Irinotecan: A Potential Implant to Hinder Recurrence of Glioblastoma Multiforme

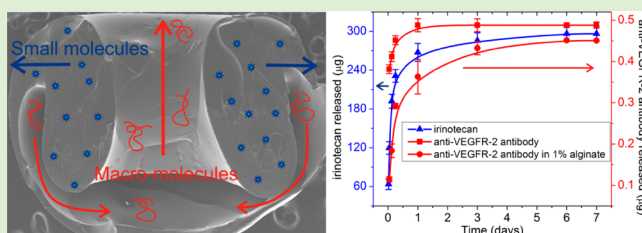
Vishal Sharma,[†] Melanie Köllmer,[‡] Magdalena Szymusiak,[†] Ludwig C. Nitsche,[†] Richard A. Gemeinhart,^{‡,§,||} and Ying Liu^{*,†,‡}

[†]Department of Chemical Engineering and [§]Department of Bioengineering, University of Illinois at Chicago, Chicago, Illinois 60607, United States

[‡]Department of Biopharmaceutical Sciences and ^{||}Department of Ophthalmology and Visual Sciences, University of Illinois, Chicago, Illinois 60612, United States

Supporting Information

ABSTRACT: Heterogeneous toroidal-spiral particles (TSPs) were generated by polymer droplet sedimentation, interaction, and cross-linking. TSPs provide a platform for encapsulation and release of multiple compounds of different sizes and physicochemical properties. As a model system, we demonstrate the encapsulation and independently controlled release of an anti-VEGFR-2 antibody and irinotecan for the treatment of glioblastoma multiforme. The anti-VEGFR-2 antibody was released from the TS channels and its binding to HUVECs was confirmed by confocal microscopy and flow cytometry, suggesting active antibody encapsulation and release. Irinotecan, a small molecule drug, was released from the dense polymer matrix of poly(ethylene glycol) diacrylate (MW ~ 700 g/mol; PEGDA 700). Released irinotecan inhibited the proliferation of U251 malignant glioma cells. Since the therapeutic compounds are released through different pathways, specifically diffusion through the polymer matrix versus TS channels, the release rate can be controlled independently through the design of the structure and material of particle components.



INTRODUCTION

Treatment of complex diseases often requires the simultaneous delivery of multiple therapeutic agents at optimum administration rates for a synergistic effect.¹ The goal of developing vehicles to codeliver multiple therapeutic agents is a significant driver of research.^{2–4} Manipulating the release of multiple therapeutic agents independently of one another is beneficial for drug synergy. However, this can be a difficult task when the therapeutic agents have distinct physicochemical properties, such as size, hydrophobicity, and stability.⁵ For example, many typical small molecule drugs used for chemotherapy are hydrophobic, while larger proteins and peptides are hydrophilic. Proteins must be protected from degradation and denaturing before they reach the target site. These two types of therapeutic agents require independent encapsulation and dosing techniques. Therefore, it is desirable to design and synthesize novel heterogeneous particles that are able to encapsulate and release multiple compounds. Furthermore, the methods should have the flexibility to deal with a wide spectrum of physicochemical properties and independently tunable release rates of the compounds.

We previously developed a method for self-assembling heterogeneous toroidal-spiral particles (TSPs) that contributed a tunable internal structure, in addition to a polymeric matrix, to provide a second pathway for drug encapsulation and

release.⁶ Short chain PEGDA was chosen as the material of the main polymer matrix, which only allows diffusion of small molecule drugs and confines macromolecules to the intricate spiral channels.^{7–12} Encapsulated therapeutic macromolecules are released only by diffusion through the TS channels.⁶ PEG has been approved by the FDA for a variety of biomedical applications and PEGDA-based hydrogel has been widely used in tissue engineering.^{13,14} In this study, we apply TSPs to encapsulate and independently release anti-VEGFR-2 antibody and irinotecan, which is a drug combination currently used for treating glioblastoma multiforme (GBM). The current size of the TSP is millimeter scale, which can be used for postsurgical implant or administered using catheters.

GBM is the most aggressive form of primary brain tumor and is ultimately fatal.¹⁵ Standard treatments include surgical removal of the tumor, postsurgical chemotherapy, and radiotherapy to prevent recurrence.¹⁶ However, recurrence is probable, with a median survival time of approximately one year.¹⁷ Through the use of chemotherapy following resection, recurrence of tumors can be delayed by inhibiting proliferation of metastatic cells not excised. Several implanted systems have

Received: October 18, 2013

Revised: January 23, 2014

Published: January 26, 2014

been designed to locally deliver chemotherapeutic agents directly to the brain, bypassing difficulties of crossing the blood–brain barrier by systemic administration.¹⁸ The postsurgical implantation, at the site of neoplasm, of biodegradable polymeric wafers (Gliadel) incorporating a single anticancer drug, carmustine, was approved by the FDA in 1996 to prevent GBM recurrence.¹⁹ However, treatment of complex diseases usually requires synergistic delivery of multiple compounds to shut down multiple disease pathways. Addition to anticancer drugs, such as irinotecan, growth factor inhibitors has recently attracted attention in inhibiting malignant gliomas.²⁰ Vascular endothelial growth factor (VEGF) promotes angiogenesis and is highly up-regulated in GBM.^{21,22} The development of new vasculature at the tumor site supplies the demand for nutrients by malignant cells and plays a vital role in tumor growth of new metastatic foci. VEGF binds to receptors that are selectively expressed on endothelial cells: VEGFR-1 (flt-2), VEGFR-2 (flk-1), and VEGFR-3 (flt-4). It has been well established that VEGFR-2 is primarily responsible for the angiogenic effects of VEGF.²³ Many reports have documented that the administration of anti-VEGF antibodies, along with the anticancer drug irinotecan, leads to prohibit GBM progression.^{24–27}

The TSP can incorporate small molecule drugs into the dense polymer matrix and encapsulate macromolecules into the TS channels. Therefore, TSPs allow for multiple compounds to release through independent pathways and the release rates of the compounds can be manipulated separately to reach drug synergy. The release of small molecule drug from the main polymer matrix can be controlled by the mesh size of the polymer, which is affected by polymer concentration and cross-link density.^{28,29} The TS channels, through which the macromolecules diffuse, can be a different polymeric phase whose material properties can be adjusted independently. In addition, the structure (such as length and width) of the TS channels can be varied to further fine-tune release rates of the macromolecules. Moreover, formation of TSPs is through a single-step process of drop interaction and solidification in an aqueous solution, which represents benign conditions to preserve sensitive protein structure and functionality. In this paper, we report the release of both irinotecan and anti-VEGFR-2 antibody from the same TSP. The *in vitro* experiments showed that the released anti-VEGFR-2 antibody has receptor-specific binding with the HUVEC membrane, which proves that the bioactivity of the protein has been preserved during the encapsulation and release. The release of irinotecan onto U251 malignant glioma cells prevented their proliferation for approximately one week at 300 μg drug loading in 20 particles. We expect the release of the two compounds from the same TSPs would simultaneously shut down the angiogenic pathway and disrupt DNA replication to hinder recurrence of GBM.

■ EXPERIMENTAL SECTION

Materials and Reagents. Irgacure 2959 (2-hydroxy-1-[4-(2-hydroxyethoxy) phenyl]-2-methyl-1-propanone; I-2959) was kindly provided by Ciba Specialty Chemicals (Basel, Switzerland). PEGDA 700, alginate sodium salt from brown algae (low viscosity), glycerol, paraformaldehyde, ethanol, bisbenzimidazole H 33258, Dulbecco's phosphate buffered saline (DPBS) with CaCl_2 and MgCl_2 , fetal bovine serum (FBS), calcium chloride hexahydrate, sodium azide, and irinotecan hydrochloride were purchased from Sigma-Aldrich (St. Louis, MO). Fluorescence activated cell sorter (FACS) buffer was prepared as 1% PBS, 5% FBS, and 0.05% 3 M NaN_3 . Human U251

malignant glioma (U251 MG) cells were a kind gift from Dr. Lena Al-Harhi at Rush University and were cultured in DMEM (Corning, NY) supplemented with 5% FBS. HUVECs and EBM-2 medium along with supplements and growth factors for the cells were purchased from Lonza (Walkersville, MD). Alexa Fluor 647 conjugated mouse antihuman CD309 (VEGFR-2) antibody and Alexa Fluor 647 mouse IgG1 (κ isotype control; FC) antibody were purchased from Biolegend (San Diego, CA). MTS cell proliferation assay was purchased from Promega (Madison, WI). Water used in all experiments was deionized to 18.2 $\text{M}\Omega\text{-cm}$ (Nanopure II, Barnstead, Dubuque, IA). All chemicals were purchased at standard grades and used as received.

TSP Formation. TSPs were prepared by solidifying liquid droplet structure during droplet sedimentation and interaction through a stratified aqueous solution, modifying the procedure that we have previously reported.^{6,30} Briefly, a polymeric drop, consisting of low molecular weight PEGDA and irinotecan, was dropped into a bulk solution of similar viscosity. This was followed by the introduction of a second drop consisting of anti-VEGFR-2 antibody solution with or without sodium alginate (1% by weight). Specifically, the leading drop phase contained 83% PEGDA 700, 14% DMSO, 3% I-2959 by weight, and 3 mM irinotecan. The trailing drop phase consisted of 0.24 μM anti-VEGFR-2 antibody, 45% glycerol, and 55% PBS buffer by weight. To further hinder the release of anti-VEGFR-2 antibody, sodium alginate of 1% in the final solution was added to the trailing drop. The top layer of the bulk solution consisted of 50% glycerol, 40% DI water, and 10% EtOH by weight, while the bottom layer of the bulk solution consisted of 60% glycerol, 30% DI water, and 10% CaCl_2 by weight. The high viscosity of the bulk solution, which reduces molecular diffusivity and suppresses currents, helps to maintain the salt gradient. All solutions are miscible and the interfacial tension was negligible compared to viscous forces. During drop sedimentation, the nonlinear interaction of the drops causes drop catch-up and recirculation of entrained liquid which results in the well-defined toroidal-spiral channel.⁶ When the droplets evolved into the appropriate structures (observed through the high-speed camera), the PEGDA droplet was polymerized by high-intensity UV light exposure ($\sim 10 \text{ W/cm}^2$). The resulting particles settled further through the bottom layer of the bulk solution, where CaCl_2 ionically cross-linked the alginate contained in the trailing drop. Finally, the particles were rinsed with DI water and placed into FACS buffer at pH 7.4 for *in vitro* release measurements at 37 $^\circ\text{C}$.

Droplet volume (8.5 μL) was controlled by using syringe pumps. Two needles were placed next to each other with the tip of one needle positioned slightly lower (Figure 1a). This allowed for both drops to fall from the same needle tip. With the two needles close enough, the secondary drop vertically aligned with the leading drop ensuring the axisymmetric structure of the TSPs. The structural evolution of the TSPs was recorded using a high-speed camera (Allied Vision Technology, Prosilica GX 1050, Germany) with a magnification lens (MLG-10X, Computar, Commack, NY). Representative evolutionary stages of the TSP formation by droplet interaction and sedimentation are presented in Figure 1b.

Release of Anti-VEGFR-2 Antibody. Anti-VEGFR-2 antibody was encapsulated in the channels of the TSPs. Two TSPs were placed into 100 μL FACS buffer at 37 $^\circ\text{C}$. At specific time points (1, 3, 6, 24, 72, 144, 168 h), buffer was collected and replaced with fresh buffer. Fluorescence intensities of the collected buffer solutions were measured at an excitation and emission wavelength of 633 and 666 nm, respectively (Fluoroskan II, LabSystems, Franklin, MA). The measured intensities were compared to a calibration curve to quantify the amount of anti-VEGFR-2 antibody released from the TSPs into the buffer solutions.

Release of Irinotecan. Release of irinotecan from the PEGDA polymer matrix of the TSP was measured in 500 μL of DMEM at 37 $^\circ\text{C}$. Based on preliminary experiments, approximately 15 μg of irinotecan was released per particle over a week. A total of 20 and 10 TSPs were used for releasing 300 and 150 μg of irinotecan, respectively. Particles of similar geometry were produced with no irinotecan encapsulated as a negative control. For the release studies,

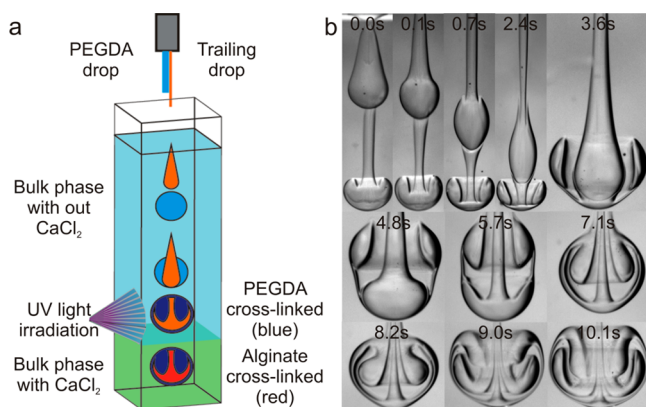


Figure 1. Formation of TSP by droplet interaction, sedimentation, and cross-linking. (a) Schematic drawing of TSP formation. When the desired TSP structure (such as TS channel length and position) was observed, PEGDA was rapidly cross-linked by UV light, which prevented further progression of the channels. The resulting particle settled further through the bottom layer of the bulk solution, where CaCl_2 ionically cross-linked the alginate contained in the trailing drop. (b) High speed camera images depicting the evolutionary stages of TSP formation. The radius of the fused drops was 1 mm.

all of the DMEM was collected and replaced with 500 μL of fresh media at specific time points (0.5, 1, 3, 6, 24, 72, 144, 168 h). Absorbance of collected DMEM buffer solutions was measured at 370 nm using Shimadzu 1601 UV spectrophotometer (Tokyo, Japan) and compared to a calibration curve to quantify the amount of irinotecan released into the buffer solutions.

Encapsulation Efficiency. The encapsulation efficiency of the drugs (irinotecan or anti-VEGFR-2 antibody) was calculated as the ratio of the drug released from a single TSP at the end of release measurements over a week and the amount of drug initially dissolved in one droplet before solidification. Basing efficiency upon release as opposed to loading (before release) makes this a particularly stringent measure. The initial concentrations of irinotecan (in the leading drop) and anti-VEGFR-2 antibody (in the trailing drop) were 3 mM and 0.24 μM , respectively. The volume of the droplets was approximately 8.5 μL .

Immunofluorescence of Anti-VEGFR-2 Antibody Bound to HUVECs. Alexa Fluor 647 tagged anti-VEGFR-2 antibody was allowed to release from a single TSP for 24 h into 100 μL of FACS buffer with 1% BSA at 37 $^\circ\text{C}$.³¹ A TSP with similar structure encapsulating the same concentration of isotype control was also generated. HUVECs (20000/well) were incubated overnight in 200 μL of medium in wells of a chambered coverglass (Lab-Tek II 1.5). Medium was removed and cells were rinsed with PBS. Then cells were fixed with 2%

paraformaldehyde for 15 min and 4% paraformaldehyde for 15 min subsequently. Cells were treated with 200 μL of blocking solution (FACS buffer with 1% BSA) for 30 min on a shaker. A total of 100 μL of the blocking solution was removed and 100 μL of FACS buffer containing the released anti-VEGFR-2 antibody or its isotype control was added. The cells were incubated for 3 h on a shaker. Nuclei were counterstained with bisbenzimidazole H 33258 at a final concentration of 0.1 $\mu\text{L}/\text{mL}$, which was added at the last 15 min of incubation. Cells were rinsed with DPBS and observed under confocal microscope (LSMS10 Meta, ZEISS, Jena, Germany). Images were analyzed with LSM510 Meta software (v4.2).

Measurements of Anti-VEGFR-2 Antibody Binding to HUVECs. Anti-VEGFR-2 antibody was allowed to release from two TSPs into FACS buffer at 37 $^\circ\text{C}$. Buffer was collected at specific time points (1, 3, 6, 24, 72, 144, 168 h) and stored at 4 $^\circ\text{C}$ until incubated with cells. The same amount of fresh FACS buffer was added back to the sample after collections to maintain the volume of the release media. A total of 100000 HUVECs were washed with 500 μL of FACS buffer. Cells were centrifuged for 5 min at 1000 rpm and supernatant was removed. HUVECs were incubated for 30 min within 100 μL of collected buffer solution containing the released anti-VEGFR-2 antibody or its isotype control. Cells were then centrifuged for 5 min at 1000 rpm and the supernatant was removed, followed by two stages of washing with 500 μL of FACS buffer to remove unbound anti-VEGFR-2 antibody.^{32,33} The cell suspension was added into flow cytometry tubes (BD Falcon 12 \times 75 mm tube with 35 μL cell strainer cap) and analyzed using a flow cytometer (CyAn ADP, Beckman Coulter, Fullerton, CA) with Summit software v4.3 (Beckman Coulter, Fullerton, CA).

Cell Viability. Irinotecan was released from 10 or 20 TSPs into DMEM buffer at 37 $^\circ\text{C}$ over the course of 168 h. Buffer solutions were collected at specific time points (0.5, 1, 3, 6, 24, 72, 144, 168 h) and replaced with an equal volume of fresh DMEM. U251 MG cells were seeded into a 96-well plate at a density of about 3500 cells/well.³⁴ Cells were placed in an incubator at 37 $^\circ\text{C}$ and 5% CO_2 for 48 h or until cells reached approximately 80% confluence, at which point the media was removed and replaced with the collected buffer containing the released irinotecan. Negative control had fresh DMEM without irinotecan while positive controls had various concentrations of irinotecan directly dissolved in DMEM. Cells were allowed to proliferate in an incubator for 72 h. Cells were then rinsed with DPBS and MTS reagent was added to the wells following the Promega protocol. Reaction was allowed for 3 h and absorbance was read at 492 nm using an absorbance plate reader (Labsystems Multiskan Plus, Fisher Scientific Inc., Hampton, NH). Relative proliferation was presented as the absorbance of the sample divided by the absorbance of the negative control with the MTS blank subtracted.

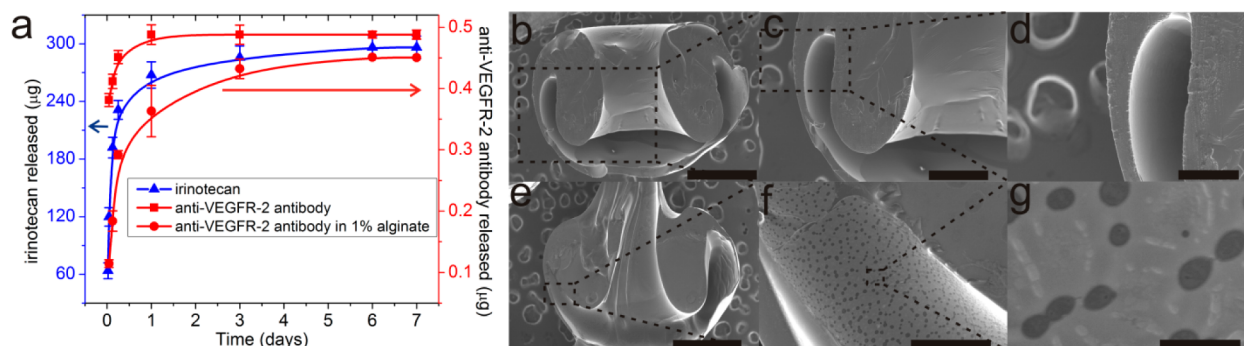


Figure 2. (a) Release of irinotecan and anti-VEGFR-2 antibody with and without incorporation of alginate in TS channels. Each point represents the mean plus or minus the standard deviation ($n = 3$). (b–d) Scanning electron microscope (SEM) images of representative internal structures of TSPs not incorporating alginate into the channels. Scale bars are 1 mm (b), 500 μm (c), and 250 μm (d). Representative SEM images of the TSP made with alginate incorporated into the channels (e, f). (g) Porous structure of alginate. Scale bars are 1 mm (e), 100 μm (f), and 10 μm (g).

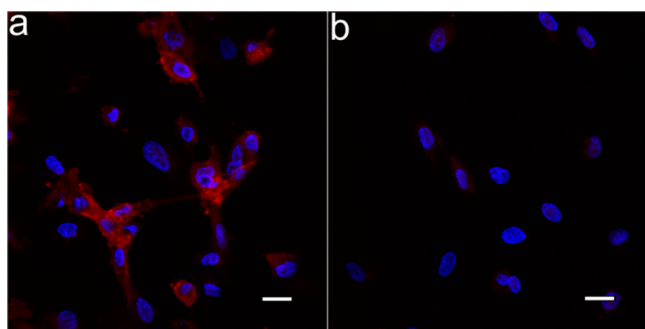


Figure 3. Confocal microscopy images of antibody binding to HUVECs. (a) Anti-VEGFR-2 antibody (red) attachment to HUVECs. Nucleus was dyed blue for ease of interpretation. (b) Isotype control showed minimal attachment to HUVECs. Scale bars are 20 μm .

RESULTS AND DISCUSSION

Independent Release of Multiple Compounds. Motivated by current approaches to the treatment of glioblastoma multiforme and other cancers using the combination of anti-VEGFR-2 antibody and irinotecan, these two compounds were encapsulated in the TSPs. The self-assembly process to form TSPs has high drug encapsulation efficiency. The drug encapsulation efficiency for anti-VEGFR-2 antibody was $79.7 \pm 1.2\%$ without the presence of alginate in the channels and $73.6 \pm 1.1\%$ with the presence of 1% alginate in the channels. The encapsulation efficiency for irinotecan was $92.9 \pm 3.7\%$. Potential reasons for the loss of the drugs are (1) diffusion of therapeutic compounds into the bulk solution during sedimentation, (2) drug that is not released from the particles, (3) loss during particle rinsing, and (4) exclusion of the long tail from the particle upon solidification. The main limitation

on encapsulation efficiency seems to be formation and cutoff of the long tail by the surrounding bulk fluid upon cross-linking (Figure 1b). The encapsulation efficiency was always higher for irinotecan compared to anti-VEGFR-2 antibody because the tails formed by the trailing drop was generally bigger than the tails formed by the leading drop (Figure 1b). Based on the efficient loading, it is possible to have significant control of the release.

It is ideal to control the release rates independently in order for the compounds to work synergistically at the targeting site. However, due to their difference in size, it is difficult to release the small molecule and macromolecule independently from one single device.³⁵ Currently, the release of multiple compounds is mainly controlled by polymer degradation, molecular diffusion, or a combination of both. If the release rate is controlled by polymer degradation, then all the compounds are essentially released at the same rate; if controlled by diffusion, the smaller molecules will be released much faster. The heterogeneous TSPs allow independent tuning of multiple parallel pathways of drug release.

In this study, the larger protein molecule, anti-VEGFR-2 antibody, was loaded into the TS channels, while irinotecan was preblended into the main polymer matrix, which consists of high concentration of PEGDA 700. The high concentration of PEGDA allows for rapid photo-cross-linking (on the millisecond time scale) and subsequent formation of dense polymer matrix. The mesh size of the polymer (approximately 3 nm)¹¹ allowed slow diffusion of irinotecan and prevented permeation of anti-VEGFR-2 antibody (molecular size of approximately 150 kDa with radius of gyration approximately 5 nm).³⁶ Anti-VEGFR-2 antibody was released by diffusion through the curved TS channels; it is possible that osmotic pressure differences affect this release rate, which we will examine in the

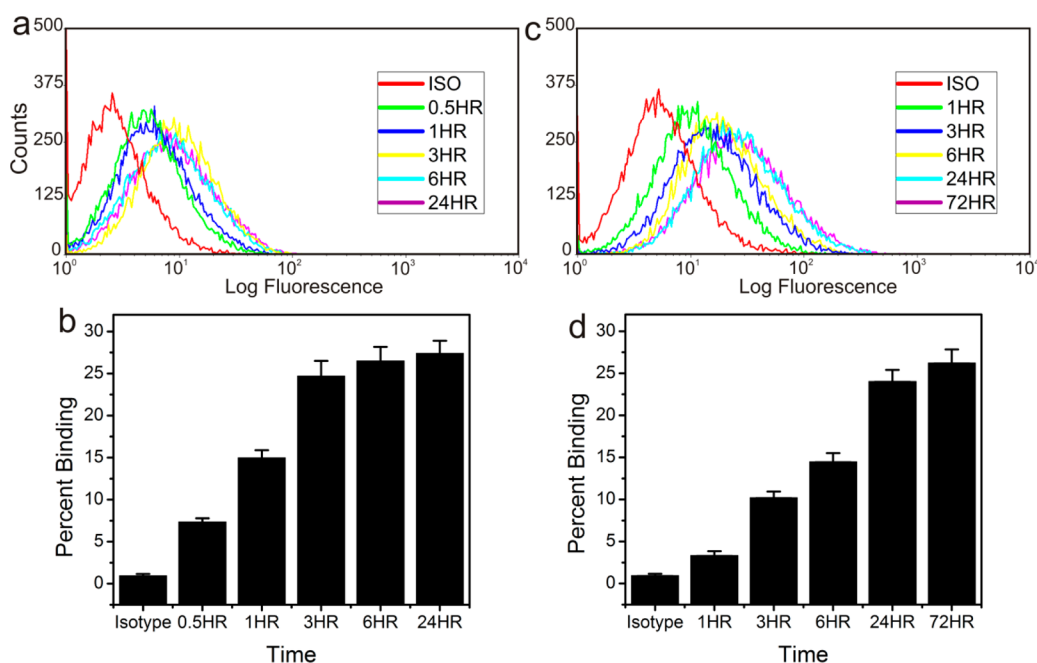


Figure 4. Flow cytometry measurements of anti-VEGFR-2 antibody binding to HUVECs. (a) Anti-VEGFR-2 antibody released from TS channels without alginate showed similar fluorescence from the cells for time points after 3 h (representative data acquired from one sample run). (b) Percent cells bound with the antibody were similar for release times beyond three hours. (c) For TSPs fabricated with alginate in the channels, the fluorescence from the cells increased with longer time of release up to 72 h (representative data acquired from one sample run). (d) The percent cells bound with the antibody increased over time up to 72 h. The isotype control for each case showed minimal binding. Each data point represents the mean plus or minus the standard deviation of three independent samples.

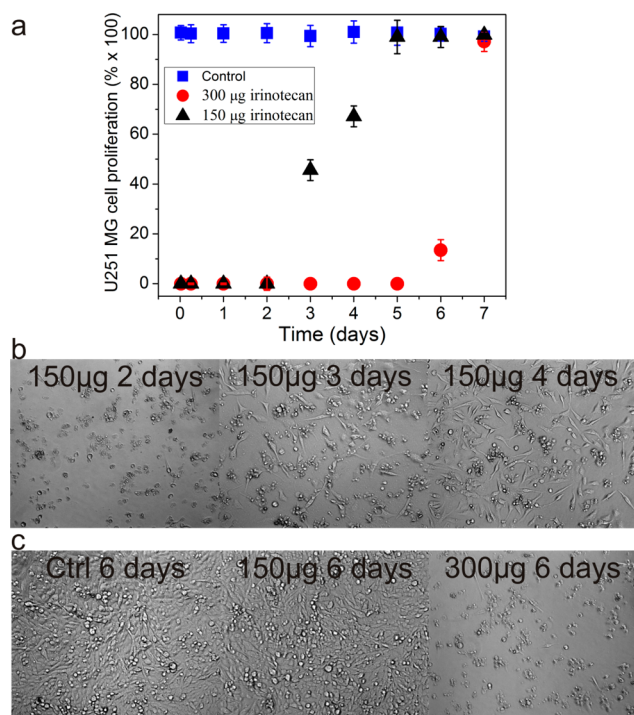


Figure 5. Inhibition of U251 MG cell growth by sustained release of irinotecan from TSPs. (a) Relative proliferation of U251 MG cells for 7 days. After the first 24 h, the release media was collected and replaced every 24 h. Therefore, the media only contained irinotecan released after the last collection within 24 h. (b) Representative images of U251 MG cells after being treated with media containing irinotecan released on the second, third, and fourth days. The total drug loading is 150 µg in 10 TSPs. (c) Images of U251 cells treated with release media from the sixth day of release containing no irinotecan (left), irinotecan released from 10 TSPs (middle), and irinotecan released from 20 TSPs (right). The drug loading in one TSP was about 15 µg.

future. By changing the material composition (empty channel vs low concentration alginate hydrogel) in the TS channels, release of the anti-VEGFR-2 antibody was manipulated from a few hours to a few days (Figure 2a). In the first case, anti-VEGFR-2 antibody was dissolved in an aqueous solution without any polymer. When the main polymer matrix of PEGDA was cross-linked, anti-VEGFR-2 antibody was encapsulated in empty TS channels (Figure 2b–d), through which the release of anti-VEGFR-2 antibody reached approximately 80% after 3 h. In the second case, 1% sodium alginate was added to the aqueous drop phase containing anti-VEGFR-2 antibody. Alginate forms a porous structure in the TS channels to further prolong the release of anti-VEGFR-2 antibody (Figure 2e–g). Cross-linked alginate inside the channels produced large pores with an average size of about 3 µm (Figure 2g), which allows for the complete release of the protein. In this case, the release took more than 3 days to reach 80% and continued for several more days.

In Vitro Activity of the Anti-VEGFR-2 Antibody Released from TSPs. The activity of the protein was characterized by the binding of antibody to receptors on human vascular cells, that is, HUVECs. The binding of anti-VEGFR-2 antibody with HUVECs was confirmed by confocal microscopy (Figure 3). When active anti-VEGFR-2 antibody is bound to the receptor on the cell membrane, the fluorescence can be observed from the cell membranes. If antibodies are denatured, they are unable to bind to their native ligands in a

specific manner. Confocal microscopy confirmed that anti-VEGFR-2 antibody remained active through the TSP-fabrication process (Figure 3). The isotype control showed minimum binding when compared to the anti-VEGFR-2 antibody (Figure 3b), indicating that the binding was specific to the ligand.

Flow cytometry was used to quantify the binding to HUVECs of the anti-VEGFR-2 antibody cumulatively released from two TSPs at certain time points. It was determined that the released antibody kept the same cell binding capacity as the original unprocessed anti-VEGFR-2 antibody in solution (Supporting Information, Figure 1). Collected buffer solutions from later stages of the release show increased cell binding. This indicates that significant release is still occurring at these times as fresh media was added after each time point. For TSPs with empty channels (without the incorporation of sodium alginate), most of the binding occurred within the first 3 h (Figure 4). With the incorporation of 1% sodium alginate into the TS channels, release of the anti-VEGFR-2 antibody was hindered by the polymer and a similar binding required 72 h of release (Figure 4d). This corresponded well with the release rate for the anti-VEGFR-2 antibody (Figure 2a). Release of the same concentration of isotype control from the TSPs was monitored for the same time period and exhibited minimal binding to cells at any time (Figure 4a,b). This indicates that the anti-VEGFR-2 antibody has bound with HUVECs through VEGFR-2 expressed on the cells. Therefore, the bioactivity of the released antibody was preserved through the TSP fabrication process.

In Vitro Activity of Released Irinotecan. The activity of irinotecan released from the TSP to hinder the proliferation of U251 malignant glioma cells is demonstrated. The toxicity of irinotecan was initially measured to determine the concentration required for irinotecan to effectively hinder cell growth (Supporting Information, Figure 2). Based on this concentration and the previously measured irinotecan release rate, we were able to decide the loading of irinotecan into the polymer matrix of the TSPs. Cells were monitored visually and the metabolic activity of the cells was characterized using MTS assay. With 150 µg irinotecan released from 10 TSPs, cell growth was effectively inhibited for 2 days (Figure 5a), which is evidenced by severe cell morphologic change and lower cell number (Figure 5b). With twice the number of particles used, inhibition lasted six days (Figure 5c). In response to the release of the next 24 h, cell proliferation was almost 100% as remaining irinotecan was not sufficient to inhibit the cell growth. All negative control samples exhibited no hindering effect on cell growth, indicating the drug carrier (TSPs without drug) was nontoxic to the cells (Figure 5a). Although free radicals formed by photoinitiators may be considered toxic to cells,³⁷ the cross-linking involved in TSP formation evidently consumes the majority of free radicals during polymerization. Furthermore, irinotecan was not degraded by UV exposure during droplet solidification, which is evident by the similar UV absorbance (Supporting Information, Figure 3) of pure irinotecan and irinotecan irradiated with UV light.

CONCLUSION

Herein, we presented the formation of TSPs encapsulating irinotecan (small molecule, 587 Da) and anti-VEGFR-2 antibody (macromolecule, ~150 kDa) as a drug combination for treatment of GBM. Independent modes of release were achieved for the two compounds. The bioactivities of both

drugs were maintained throughout the fabrication process. The macromolecule was loaded into the TS channels by droplet sedimentation and interaction. The small molecule drug was preblended in the precursor polymer solution. Release rates of the macromolecules were modulated by the addition of sodium alginate to the TSP channels, increasing from 3 h to 3 days for 80% release. Small molecule chemotherapeutic drug with 300 μg loaded into a dense PEGDA 700 polymer matrix sustained release for approximately one week. The independent manipulation of the release rates for two compounds was demonstrated in vitro. Systematic tuning of TSP structure, guided by in vivo measurements of drug release and activity, to optimize drug synergy certainly merits more investigation in the future.

The encapsulation in different regions in the single TSP and release through independent pathways resolve any potential problems in dealing with incompatibility of multiple drugs. The particle formation process is benign to delicate proteins and peptides. The TSP technology described in this paper would have broader implications for treatment of complex diseases, insofar as these require multiple therapeutic compounds with various physicochemical properties.

■ ASSOCIATED CONTENT

■ Supporting Information

Log fluorescence of anti-VEGFR-2 antibody released TSP and pure anti-VEGFR-2 antibody. Irinotecan toxicity to U251 MG cells. Absorbance of irinotecan irradiated with UV light and irinotecan alone at 370 nm. This material is available free of charge via the Internet at <http://pubs.acs.org>.

■ AUTHOR INFORMATION

■ Corresponding Author

*Tel.: +1(312) 996-8249. Fax: +1(312) 996-0808. E-mail: liuying@uic.edu.

■ Notes

The authors declare no competing financial interest.

■ ACKNOWLEDGMENTS

The methodology to form TSPs by multiple drop sedimentation and interaction was established through the support of NSF-EAGER Award (NSF-CBET 1039531). The quantitative measurements of the drug release and functionality has been funded by Chancellor's Discovery Award and Center for Clinical and Translational Science (CCTS) Award from the University of Illinois at Chicago. CCTS is supported by the NCR (UL1 TR000050) and the National Institute for Neurologic Disorders and Stroke (NS055095). This investigation was conducted in part in a facility constructed with support from Research Facilities Improvement Program Grant (RR15482) from the National Centre for Research Resources of the National Institutes of Health (NIH). The authors thank Mary Tang and Dr. Jerry White for technical assistance.

■ REFERENCES

- (1) Mi, Y.; Zhao, J.; Feng, S.-S. *J. Controlled Release* **2013**, *169* (3), 185–192.
- (2) Wei, L.; Cai, C.; Lin, J.; Chen, T. *Biomaterials* **2009**, *30* (13), 2606–2613.
- (3) Lei, C.; Cui, Y.; Zheng, L.; Kah-Hoe Chow, P.; Wang, C.-H. *Biomaterials* **2013**, *34* (30), 7483–7494.
- (4) Shin, S.-H.; Lee, J.; Lim, K. S.; Rhim, T.; Lee, S. K.; Kim, Y.-H.; Lee, K. Y. *J. Controlled Release* **2013**, *166* (1), 38–45.

- (5) Liu, D.; Bimbo, L. M.; Mäkilä, E.; Villanova, F.; Kaasalainen, M.; Herranz-Blanco, B.; Caramella, C. M.; Lehto, V.-P.; Salonen, J.; Herzig, K.-H.; Hirvonen, J.; Santos, H. A. *J. Controlled Release* **2013**, *170* (2), 268–278.
- (6) Szymusiak, M.; Sharma, V.; Nitsche, L. C.; Liu, Y. *Soft Matter* **2012**, *8* (29), 7556–7559.
- (7) Tauro, J. R.; Gemeinhart, R. A. *Mol. Pharmaceutics* **2005**, *2* (5), 435–438.
- (8) Tauro, J. R.; Gemeinhart, R. A. *Bioconjugate Chem.* **2005**, *16* (5), 1133–1139.
- (9) Tauro, J. R.; Lee, B.-S.; Lateef, S. S.; Gemeinhart, R. A. *Peptides* **2008**, *29* (11), 1965–1973.
- (10) Elbert, D. L.; Pratt, A. B.; Lutolf, M. P.; Halstenberg, S.; Hubbell, J. A. *J. Controlled Release* **2001**, *76* (1), 11–25.
- (11) Cruise, G. M.; Scharp, D. S.; Hubbell, J. A. *Biomaterials* **1998**, *19* (14), 1287–1294.
- (12) Watkins, A. W.; Anseth, K. S. *Macromolecules* **2005**, *38* (4), 1326–1334.
- (13) Peppas, N. A.; Keys, K. B.; Torres-Lugo, M.; Lowman, A. M. *J. Controlled Release* **1999**, *62* (1), 81–87.
- (14) Burdick, J. A.; Anseth, K. S. *Biomaterials* **2002**, *23* (22), 4315–4323.
- (15) Krex, D.; Klink, B.; Hartmann, C.; von Deimling, A.; Pietsch, T.; Simon, M.; Sabel, M.; Steinbach, J. P.; Heese, O.; Reifenberger, G.; Weller, M.; Schackert, G.; Network, f. t. G. *Brain* **2007**, *130* (10), 2596–2606.
- (16) Stupp, R.; Mason, W. P.; Van Den Bent, M. J.; Weller, M.; Fisher, B.; Taphoorn, M. J.; Belanger, K.; Brandes, A. A.; Marosi, C.; Bogdahn, U. *N. Eng. J. Med.* **2005**, *352* (10), 987–996.
- (17) Smith, J. S.; Jenkins, R. B. *Front. Biosci.* **2000**, *5* (1), 213–231.
- (18) Moses, M. A.; Brem, H.; Langer, R. *Cancer Cell* **2003**, *4* (5), 337–341.
- (19) Burton, E.; Prados, M. *Curr. Treat. Options Oncol.* **2000**, *1* (5), 459–468.
- (20) Arko, L.; Katsyv, I.; Park, G. E.; Luan, W. P.; Park, J. K. *Pharmacol. Ther.* **2010**, *128* (1), 1–36.
- (21) Plate, K. H.; Breier, G.; Weich, H. A.; Risau, W. *Nature* **1992**, *359* (6398), 845–848.
- (22) Ferrara, N.; Davis-Smyth, T. *Endocr. Rev.* **1997**, *18* (1), 4–25.
- (23) Ferrara, N.; Gerber, H. P.; LeCouter, J. *Nat. Med.* **2003**, *9* (6), 669–676.
- (24) Bokstein, F.; Shpigel, S.; Blumenthal, D. T. *Cancer* **2008**, *112* (10), 2267–2273.
- (25) Kang, T.; Jin, T.; Elinzano, H.; Peereboom, D. *J. Neuro-Oncol.* **2008**, *89* (1), 113–118.
- (26) Vredenburgh, J. J.; Desjardins, A.; Herndon, J. E.; Marcello, J.; Reardon, D. A.; Quinn, J. A.; Rich, J. N.; Sathornsumetee, S.; Gururangan, S.; Sampson, J.; Wagner, M.; Bailey, L.; Bigner, D. D.; Friedman, A. H.; Friedman, H. S. *J. Clin. Oncol.* **2007**, *25* (30), 4722–4729.
- (27) Friedman, H. S.; Prados, M. D.; Wen, P. Y.; Mikkelsen, T.; Schiff, D.; Abrey, L. E.; Yung, W. K. A.; Paleologos, N.; Nicholas, M. K.; Jensen, R.; Vredenburgh, J.; Huang, J.; Zheng, M.; Cloughesy, T. J. *Clin. Oncol.* **2009**, *27* (28), 4733–4740.
- (28) Hoffman, A. S. *Adv. Drug Delivery Rev.* **2012**, *64* (Supplement (0)), 18–23.
- (29) Ross, A. E.; Tang, M. Y.; Gemeinhart, R. A. *AAPS J.* **2012**, *14* (3), 482–490.
- (30) Sharma, V.; Szymusiak, M.; Shen, H.; Nitsche, L. C.; Liu, Y. *Langmuir* **2011**, *28* (1), 729–735.
- (31) Gandhi, M.; Srikanth, R.; Yarin, A. L.; Megaridis, C. M.; Gemeinhart, R. A. *Mol. Pharmaceutics* **2009**, *6* (2), 641–7.
- (32) Köllmer, M.; Buhrman, J. S.; Zhang, Y.; Gemeinhart, R. A. *J. Dev. Biol. Tissue Eng.* **2013**, *5* (2), 18.
- (33) Köllmer, M.; Keskar, V.; Hauk, T. G.; Collins, J. M.; Russell, B.; Gemeinhart, R. A. *Biomacromolecules* **2012**, *13* (4), 963–973.
- (34) Keskar, V.; Mohanty, P. S.; Gemeinhart, E. J.; Gemeinhart, R. A. *J. Controlled Release* **2006**, *115* (3), 280–8.

(35) Peppas, N. A.; Bures, P.; Leobandung, W.; Ichikawa, H. *Eur. J. Pharm. Biopharm.* **2000**, *50* (1), 27–46.

(36) Kisko, K.; Brozzo, M. S.; Missimer, J.; Schleier, T.; Menzel, A.; Leppänen, V.-M.; Alitalo, K.; Walzthoeni, T.; Aebersold, R.; Ballmer-Hofer, K. *FASEB J.* **2011**, *25* (9), 2980–2986.

(37) Williams, C. G.; Malik, A. N.; Kim, T. K.; Manson, P. N.; Elisseff, J. H. *Biomaterials* **2005**, *26* (11), 1211–1218.